^{19}F NMR and Structural Evidence for Spin-State Modulation of Six-Coordinate Cobalt(II) in a Weak Field Porphyrin Ligand[1]

Valeriy V. Smirnov, Eric K. Woller, and Stephen G. DiMagno*

Department of Chemistry, University of Nebraska—Lincoln, Lincoln, Nebraska 68588-0304

Received February 10, 1998

The syntheses and characterization of [2,3,7,8,12,13,17,18-octafluoro-5,10,15,20-tetraphenylporphinato]cobalt, Co(F_8TPP), and [2,3,7,8,12,13,17,18-octafluoro-5,10,15,20-tetrakis(pentafluorophenyl)porphinato]cobalt, Co(F_{28}TPP), are reported. Co(F_{28}TPP)·2tol (tol = toluene) crystallizes in the monoclinic space group $C2/c$-C_h (No. 15) with $a = 22.1616(5)$ Å, $b = 12.0274(3)$ Å, $c = 19.9159(2)$ Å, $\beta = 110.645(1)°$, $V = 4967.6(2)$ Å^3, and $Z = 4$ {$d_{calcd} = 1.818$ g/cm^3; μ_a(Mo Kα) = 0.50 mm^{-1}}, and Co(F_{28}TPP)·2THF crystallizes in the triclinic space group $P\bar{1}$ (No. 2) with $a = 11.0691(1)$ Å, $b = 12.0451(1)$ Å, $c = 12.9558(2)$ Å, $\alpha = 62.531(1)°$, $\beta = 69.544(1)°$, $\gamma = 76.181(1)°$, $V = 1429.71(3)$ Å^3 and $Z = 1$ {$d_{calcd} = 1.700$ g/cm^3; μ_a(Mo Kα) = 0.45 mm^{-1}}. A comparison of the X-ray crystal structure data from Co(F_{28}TPP)·2tol and Co(F_{28}TPP)·2THF indicates that the porphyrin core expands dramatically (0.08 Å) in the six-coordinate complex. Optical and ^{19}F NMR spectroscopic studies of Co(F_{28}TPP) in the presence of added ligand demonstrate that spin-state modulation of the six-coordinate Co(II) center is facile. Partial population of the ^4E_g state is accessed upon coordination of the cobalt center with THF σ-donor ligands, while six-coordinate complexes with 1-methylimidazole result in complete conversion to the high spin state, as evinced by 280 ppm downfield chemical shifts for the β-fluorine resonances in the ^{19}F NMR spectrum. Co(F_{28}TPP) is the first example of a porphyrin which supports a high-spin cobalt ion.

The stereoelectronic properties of the porphyrin ligand are critical to modulating metal electrochemical potentials, d-orbital energies, spin states, and chemical reactivity in hemoproteins and iron porphyrin model systems.[2] In ferrous hemes (and model systems such as Fe(TPP)), two spin transitions ($S = 1 \rightarrow S = 2$, and $S = 2 \rightarrow S = 0$) are observed as the strength of the axial ligand field is increased. Similarly, Fe(III) porphyrins display low-, intermediate-, and high-spin states depending on the number and nature of the axial ligands. The porphyrin maintains a moderate in-plane ligand field while adjusting its core diameter in excess of 0.2 Å to accommodate both small, low-spin and large, high-spin ions.[2,3] The macrocycle's flexibility facilitates population of the $d_{x^2-y^2}$ orbital by radial expansion, enabling fine-tuning of spin states by endogenous ligands.[4] Iron's ability to access a full complement of spin states is largely responsible for the incredibly diverse chemistry observed in hemoproteins. However, for the reasons outlined below, the porphyrin ligand generally does not support facile spin transitions for iron's nearest neighbors on the periodic table.

Because of their ability to bind dioxygen, Co(II) porphyrins have received considerable study as models of heme oxygen carriers.[5] The electronic structure of Co(II) porphyrins is quite different from that of hemes; one ($^2A_{1g}$) electronic state for cobalt porphyrins is generally observed, regardless of the type and number of axial ligands. Scheidt and Gouterman have summarized the factors that make high-spin states accessible for Fe(II) and unlikely for Co(II) in porphyrin ligands.[4] Population of the $d_{x^2-y^2}$ orbital requires promotion of a dπ electron, sacrificing a full unit (Δ_o) of crystal field energy. High-spin states can only occur if this penalty is compensated by electron exchange. The magnitudes of electron exchange energies depend on the number of unpaired spins; thus, they are larger in high-spin Fe(II) ($S = 2$) than in high-spin Co(II) ($S = {}^3/_2$). If high-spin states are to be accessed by Co(II) in a porphyrin ligand, the in-plane ligand field must be substantially reduced to stabilize the $d_{x^2-y^2}$ metal-centered orbital. Enforcing radial expansion by benzannulation, as in octamethyltetrabenzoporphyrin,[6] and appending electronegative groups to render the nitrogen core less basic are two possible strategies leading to reduced field porphyrin ligands.

Recently, we and others reported the preparation and characterization of the extremely electron-deficient β-octafluoro-*meso*-tetraarylporphyrins F_8TPP and F_{28}TPP.[7,8] The combination of relatively planar structures and nonbasic nitrogen atoms of the fluorinated derivatives is unique among the β-perhalo-*meso*-tetraarylporphyrins.[9−20] Thus, β-octafluoro-*meso*-tetra-

(1) Abbreviations used in this manuscript are as follows: TPP, 5,10,15,20-tetraphenylporphyrin; F_8TPP, 2,3,7,8,12,13,17,18-octafluoro-5,10,15,20-tetraphenylporphyrin; F_{28}TPP, 2,3,7,8,12,13,17,18-octafluoro-5,10,15,20-tetrakis(pentafluorophenyl)porphyrin; TPFPP, 5,10,15,20-tetrakis-(pentafluorophenyl)porphyrin; OEP, 2,3,7,8,12,13,17,18-octaethylporphyrin; *p*-X-TPP, 5,10,15,20-tetrakis(4-X-phenyl)porphyrin; $(CN)_4$TPP, 2,7,12,17-tetracyano-5,10,15,20-tetraphenylporphyrin; *p*-OMeTPP, 5,10,15,20-tetrakis(4-methoxyphenyl)porphyrin; FDEPMP, 2-fluoro-3,8-diethyl-7,12,13,17,18-pentamethylporphyrin. Inclusion of these abbreviations within parentheses signifies that the porphyrin is doubly deprotonated.

(2) Scheidt, W. R.; Reed, C. A. *Chem. Rev.* **1981**, *81*, 543−555.
(3) Scheidt, W. R.; Lee, Y. J. *Struct. Bond.* **1987**, *64*, 1−70.
(4) Scheidt, W. R.; Gouterman, M. In *Iron Porphyrins, Part One*; Lever, A. B. P., Gray, H. B., Eds.; Addison-Wesley: Reading, MA, 1983; pp 89−139.
(5) Jones, R. D.; Summerville, D. A.; Basolo, F. *Chem. Rev.* **1979**, *79*, 139−179.
(6) Dolphin, D.; Sams, J. R.; Tsin, T. B.; Wong, K. L. *J. Am. Chem. Soc.* **1976**, *98*, 6970−6975.
(7) Woller, E. K.; DiMagno, S. G. *J. Org. Chem.* **1997**, *62*, 1588−1593.
(8) Leroy, J.; Bondon, A.; Toupet, L.; Rolando, C. *Chem. Eur. J.* **1997**, *3*, 1890−1893.
(9) Battioni, P.; Brigaud, O.; Desvaux, H.; Mansuy, D.; Traylor, T. G. *Tetrahedron Lett.* **1991**, *32*, 2893−2896.
(10) Bhyrappa, P.; Krishnan, V. *Inorg. Chem.* **1991**, *30*, 239−245.

S0020-1669(98)00156-6 CCC: $15.00
Published on Web 08/22/1998

arylporphyrins are expected to possess weaker ligand fields than are typical of unelaborated octaalkyl- or tetraarylporphyrins. Simple crystal field arguments predict a narrowing in the energy gap between the t_{2g} and e_g orbital sets and a reduction in the splitting between the $d_{x^2-y^2}$ and d_{z^2} orbital energies for metal atoms in the four-coordinate environment.[21] Furthermore, the spacing among the metal d-orbital energies should be more sensitive to axial ligation in planar electron-deficient porphyrins than in TPP. These considerations lead to the prediction that the d-orbital splittings of Co(II) in F_{28}TPP should resemble those of Fe(II) in hemes. Here we provide the first direct structural and ^{19}F NMR evidence to confirm this hypothesis.

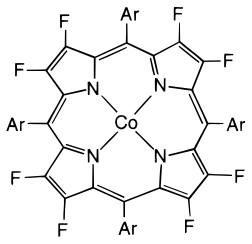

Co(F_8TPP) Ar = C_6H_5
Co(F_{28}TPP) Ar = C_6F_5

Results and Discussion

The compounds Co(F_8TPP) and Co(F_{28}TPP) were prepared under standard metalation conditions; the ligands were deprotonated with Li(HMDSA) and treated with anhydrous cobalt chloride in THF at room temperature.[22] After recrystallization from hot toluene, the metalloporphyrins were heated at 110 °C under vacuum to remove the residual solvent. The optical spectra of the fluorinated metallomacrocycles in CH_2Cl_2 exhibit hypsochromic shifts in the Soret bands (Co(F_8TPP), 398 nm; Co(F_{28}TPP), 394 nm; Co(TPP), 404 nm) and Q(1,0) bands (Co(F_8TPP), 519 nm; Co(F_{28}TPP), 520 nm; Co(TPP), 530 nm). The shifts in the absorption maxima to higher energies is also observed in the spectra of the analogous zinc complexes.[7] A strong resonance interaction of the fluorine lone pairs with the porphyrin LUMOs is the most likely explanation for the observed spectral shifts; the same effect is seen in 2,3,7,8,12,13,17,18-octamethoxyporphyrin.[23] The reduced splitting between the Soret and Q bands for Co(F_8TPP) compared to Co(F_{28}TPP) may reflect increased conjugation of the phenyl substituents, suggesting a slightly nonplanar solution structure for Co(F_8TPP). Whatever the origin of the difference between the electronic spectra of Co(F_8TPP) and Co(F_{28}TPP), the absorption spectra are not consistent with grossly nonplanar macrocycle geometries. Previous spectroscopic studies of β-perhalo-*meso*-tetraarylporphyrins have demonstrated that bathochromic shifts are observed in the ground-state electronic spectra if the macrocycle adopts a highly nonplanar conformation.[24] Thus, the hypsochromically shifted spectra obtained for Co(F_8TPP) and Co(F_{28}TPP) provide indirect evidence for macrocycle solution structures which are more planar than their octachlorinated and octabrominated counterparts.

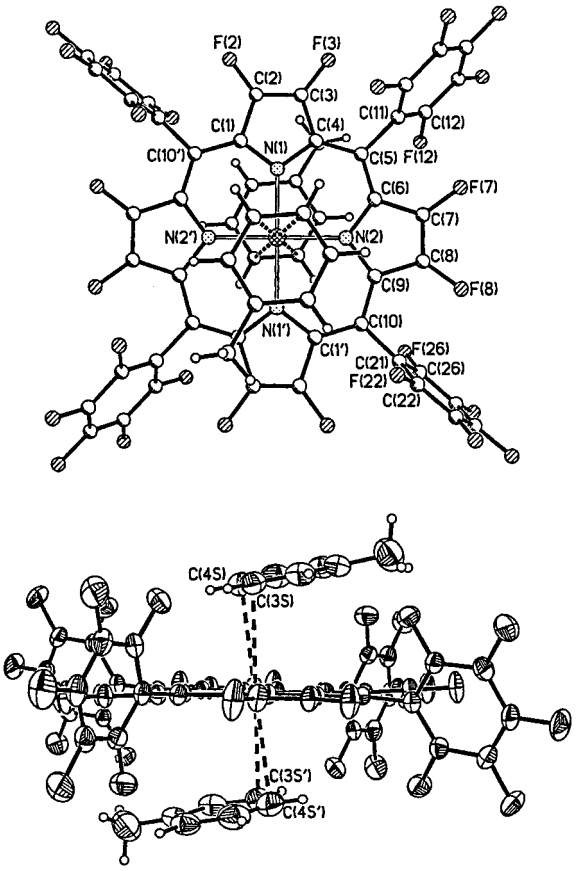

Figure 1. Perspective drawings from the X-ray crystal structure determination of Co(F_{28}TPP)·2tol. The view for the top figure is orthogonal to the porphyrin plane. The bottom figure is drawn with 50% thermal ellipsoids.

Structure of Co(F_{28}TPP)·2tol. Crystals of Co(F_{28}TPP)·2tol (tol = toluene) suitable for X-ray diffraction were obtained from toluene. Perspective drawings from the crystal structure determination are shown in Figure 1. Selected bond lengths and angles are given in Table 1, and a comparison of this structure with those of other relevant metalloporphyrins is given in Table 2. The porphyrin ring is essentially flat, and the largest deviations (0.05 Å) from the porphyrin mean plane occur at C(3) and C(10). The pentafluorophenyl groups are at an average dihedral angle of 75.7° to the mean porphyrin plane. The

(11) Birnbaum, E. R.; Hodge, J. A.; Grinstaff, M. W.; Schaefer, W. P.; Henling, L.; Labinger, J. A.; Bercaw, J. E.; Gray, H. B. *Inorg. Chem.* **1995**, *34*, 3625−3632.
(12) Ellis, P. E. J.; Lyons, J. E. *Catal. Lett.* **1991**, *8*, 45−52.
(13) Grinstaff, M. W.; Hill, M. G.; Labinger, J. A.; Gray, H. B. *Science* **1994**, *264*, 1311−1313.
(14) Grinstaff, M. W.; Hill, M. F.; Birnbaum, E. R.; Schaefer, W. P.; Labinger, J. A.; Gray, H. B. *Inorg. Chem.* **1995**, *34*, 4896−4902.
(15) Hodge, J. A.; Hill, M. G.; Gray, H. B. *Inorg. Chem.* **1995**, *34*, 809−812.
(16) Henling, L. M.; Schaefer, W. P.; Hodge, J. A.; Hughes, M. E.; Gray, H. B.; Lyons, J. E.; Ellis, P. E. J. *Acta Crystallogr.* **1993**, *C49*, 1743−1747.
(17) Lyons, J. E.; Ellis, P. E. J. In *Metalloporphyrins in Catalytic Oxidations*; Sheldon, R. A., Ed.; Marcel Dekker: New York, 1994; pp 297−324.
(18) Hoffman, P.; Labat, G.; Robert, A.; Meunier, B. *Tetrahedron Lett.* **1990**, *31*, 1991−1994.
(19) Marsh, R. E.; Schaefer, W. P.; Hodge, J. A.; Hughes, M. E.; Gray, H. B.; Lyons, J. E.; Ellis, P. E. J. *Acta Crystallogr.* **1993**, *C49*, 1339−1342.
(20) Mandon, D.; Ochsenbein, P.; Fischer, J.; Weiss, R.; Jayaraj, K.; Austin, R. N.; Gold, A.; White, P. S.; Brigaud, O.; Battioni, P.; Mansuy, D. *Inorg. Chem.* **1992**, *31*, 2044−2049.
(21) Cotton, F. A.; Wilkinson, G. *Advanced Inorganic Chemistry*; John Wiley & Sons: New York, 1980.
(22) Arnold, J.; Dawson, D. Y.; Hoffman, C. G. *J. Am. Chem. Soc.* **1993**, *115*, 2707−2713.
(23) Merz, A.; Schropp, R.; Lex, J. *Angew. Chem., Int. Ed. Engl.* **1993**, *32*, 291−293.
(24) Ochsenbein, P.; Ayougou, K.; Mandon, D.; Fischer, J.; Weiss, R.; Austin, R. N.; Jayaraj, K.; Gold, A.; Terner, J.; Fajer, J. *Angew. Chem., Int. Ed. Engl.* **1994**, *33*, 348−350.

Table 1. Selected Bond Length (Å) and Angles (deg) for Co(F_{28}TPP)·2tol and Co(F_{28}TPP)·2THF[a]

	Co(F_{28}TPP)·2tol	Co(F_{28}TPP)·2THF		Co(F_{28}TPP)·2tol	Co(F_{28}TPP)·2THF
Co−N(1)	1.9845(14)	2.071(2)	C(10)−C(1′)	1.383(2)	1.402(4)
Co−N(2)	1.9884(14)	2.064(2)	C(5)−C(11)	1.500(2)	1.499(4)
N(1)−C(1)	1.380(2)	1.375(3)	C(10)−C(21)	1.503(2)	1.505(4)
N(1)−C(4)	1.387(2)	1.374(4)	F(2)−C(2)	1.339(2)	1.343(3)
N(2)−C(6)	1.382(2)	1.378(4)	F(3)−C(3)	1.339(2)	1.347(3)
N(2)−C(9)	1.379(2)	1.370(3)	F(7)−C(7)	1.339(2)	1.343(3)
C(1)−C(2)	1.440(2)	1.444(4)	F(8)−C(8)	1.340(2)	1.338(3)
C(3)−C(4)	1.435(2)	1.445(4)	Co−O(1S)		2.204(2)
C(6)−C(7)	1.440(2)	1.445(4)	C(1S)−C(2S)	1.407(3)	
C(8)−C(9)	1.440(3)	1.447(4)	C(1S)−C(6S)	1.395(3)	
C(2)−C(3)	1.325(3)	1.341(4)	C(1S)−C(7S)	1.481(4)	
C(7)−C(8)	1.325(3)	1.342(4)	C(2S)−C(3S)	1.366(3)	
C(4)−C(5)	1.387(3)	1.402(4)	C(3S)−C(4S)	1.367(4)	
C(5)−C(6)	1.383(3)	1.406(4)	C(4S)−C(5S)	1.348(4)	
C(9)−C(10)	1.389(2)	1.404(4)	C(5S)−C(6S)	1.377(4)	
N(1)−Co−N(1′)	180.0	180.0	N(2)−C(6)−C(5)	126.3(2)	126.0(2)
N(2)−Co−N(2′)	180.0	180.0	N(2)−C(9)−C(10)	126.7(2)	126.1(3)
N(1)−Co−N(2)	89.95(6)	90.40(9)	C(1)−C(2)−C(3)	107.6(2)	107.5(2)
N(1)−Co−N(2′)	90.05(6)	89.60(9)	C(4)−C(3)−C(2)	107.9(2)	108.0(2)
C(1)−N(1)−C(4)	105.52(14)	107.9(2)	C(6)−C(7)−C(8)	107.7(2)	108.0(3)
C(6)−N(2)−C(9)	105.79(14)	107.7(2)	C(9)−C(8)−C(7)	107.7(2)	107.3(2)
N(1)−C(1)−C(2)	109.6(2)	108.4(2)	C(4)−C(5)−C(6)	123.1(2)	126.0(3)
N(1)−C(4)−C(3)	109.3(2)	108.1(2)	C(9)−C(10)−C(1′)	122.6(2)	125.5(3)
N(2)−C(6)−C(7)	109.3(2)	108.2(2)	C(5)−C(4)−C(3)	124.6(2)	125.8(3)
N(2)−C(9)−C(8)	109.4(2)	108.7(2)	C(5)−C(6)−C(7)	124.4(2)	125.8(3)
N(1)−C(1)−C(10′)	126.5(2)	125.9(2)	C(10)−C(9)−C(8)	123.9(2)	125.1(3)
N(1)−C(4)−C(5)	126.1(2)	126.1(2)	C(10)−C(1′)−C(2′)	123.9(2)	125.6(3)

[a] Symmetry transformations used to generate equivalent atoms: (′) $-x, -y, -z$.

Table 2. Average Bond Lengths (Å) and Bond Angles (deg) for Co(F_{28}TPP)·2tol, Co(F_{28}TPP)·2THF, and Selected Metalloporphyrins

param	Co(F_{28}TPP)·2tol	Co(F_{28}TPP)·2THF	Co(TPFPP)·benzene	Co(TPP)	Zn(TPP)·2THF	Zn(F_{28}TPP)·L[a]	Fe(TPP)·2THT[b]	Fe(TPP)·2THF[c]
N−M	1.986(1)	2.068(2)	1.976(5)	1.949(5)	2.057(2)	2.059(6)	1.996(3)	2.057(2)
N−C_α	1.382(2)	1.374(2)	1.374(4)	1.382(4)	1.371(4)	1.382(10)	1.384(5)	1.374(4)
C_α−C_β	1.439(2)	1.445(4)	1.425(7)	1.434(5)	1.444(5)	1.439(12)	1.435(5)	1.438(4)
C_β−C_β	1.325(3)	1.341(4)	1.317(4)	1.346(5)	1.349(4)	1.337(12)	1.336(6)	1.342(4)
C_α−C_m	1.385(3)	1.403(4)	1.372(4)	1.390(5)	1.403(4)	1.397(12)	1.391(5)	1.406(4)
C_α−N−C_α	105.7(1)	107.8(2)	105.1(3)	105.0(3)	107.0(2)	107.4(6)	105.2(3)	106.7(2)
N−C_α−C_β	109.5(2)	108.4(2)	109.8(2)	110.4(3)	109.3(3)	108.3(7)	109.9(3)	109.2(2)
N−C_α−C_m	126.4(2)	126.0(2)	125.2(2)	125.5(3)	125.8(3)	125.5(7)	125.6(3)	125.5(2)
C_α−C_β −C_β	107.7(2)	107.7(2)	107.7(4)	107.2(3)	107.2(3)	108.0(8)	107.5(3)	107.5(2)
C_α−C_m−C_α	122.9(2)	125.7(3)	124.7(3)	122.2(3)	125.0(3)	126.0(8)	124.1(3)	125.8(2)
ref	this work	this work	25	26	27	7	28	29

[a] Mixed THF and CH_3CN axial ligands were obtained. [b] Low spin. [c] High spin.

complex has two toluene molecules occupying the available coordination sites of the metal. The cobalt atom is centered roughly at the midpoint of the C(3S)−C(4S) bonds in the toluene rings and the Co−C distances are 3.05 and 3.13 Å for C(3S) and C(4S), respectively. The C(3S)−C(4S) bond is offset slightly so that the cobalt atom is situated within the toluene aromatic ring, and the plane defined by C(3S), C(4S), and Co intersects the mean porphyrin plane at an angle of 86.5°. The toluene ring is canted toward the porphyrin mean plane at an 11.9° angle. In several respects, the structure of Co(F_{28}TPP)·2tol resembles those reported for Mn(TPP)·2tol[30] and the benzene solvate of [5,10,15,20-tetrakis(pentafluorophenyl)-porphinato]Co(II) (Co(TPFPP)·benzene)[25] which exhibits a single benzene molecule π-stacked over the metal. In the structure of Mn(TPP)·2tol the centrosymmetric disposition of the two toluene rings is nearly identical to that observed for Co(F_{28}TPP)·2tol; the dihedral angle between the toluene and porphyrin planes is 10.7°, and the closest Mn−C approach is 3.05 Å. In the structure of Co(TPFPP)·benzene the closest Co−C distance is 3.09 Å and the benzene ring is canted less with respect to the porphyrin plane (6°). These data suggest a slightly stronger (although still very weak) Co−arene interaction in Co(F_{28}TPP)·2tol than in Co(TPFPP)·benzene. Consistent with this interpretation, there is evidence for bond localization in the toluene rings. The largest discrepancy in bond lengths is between C(3S)−C(4S) (1.367(4) Å) and C(4S)−C(5S) (1.348(4) Å) (Figure 1). Although this difference is small (0.019 Å), it is outside experimental error.

The four nitrogen atoms and the cobalt center are coplanar in Co(F_{28}TPP)·2tol (0.01 Å average deviation), and the cobalt−nitrogen bond lengths average 1.986 Å. The Co−N bond lengths in Co(F_{28}TPP)·2tol are long for a nominally four-coordinate Co(II) porphyrin. For comparison, the Co−N bond

(25) Kadish, K. M.; Araullo-McAdams, C.; Han, B. C.; Franzen, M. M. *J. Am. Chem. Soc.* **1990**, *112*, 8364−8368.
(26) Madura, P.; Scheidt, W. R. *Inorg. Chem.* **1976**, *15*, 3182−3184.
(27) Schauer, C. K.; Anderson, O. P.; Eaton, S. S.; Eaton, G. R. *Inorg. Chem.* **1985**, *24*, 4082−4086.
(28) Mashiko, T.; Reed, C. A.; Haller, K. J.; Kastner, M. E.; Scheidt, W. R. *J. Am. Chem. Soc.* **1981**, *103*, 5758−5767.
(29) Reed, C. A.; Mashiko, T.; Scheidt, W. R.; Spartalian, K.; Lang, G. *J. Am. Chem. Soc.* **1980**, *102*, 2302−2306.
(30) Kirner, J. F.; Reed, C. A.; Scheidt, W. R. *J. Am. Chem. Soc.* **1977**, *99*, 1093−1101.

lengths average 1.976 and 1.971 Å in the planar porphyrins Co(TPFPP)·benzene[25] and Co(OEP),[31] respectively. The N−Co bond lengths average 1.949 Å in the ruffled structure of Co(TPP),[26] consistent with the trend that core contraction is associated with ruffled conformations in porphyrins.[3] The slight radial core expansion of Co(F_{28}TPP)·2tol presages the potential for a high-spin Co(II) with $d_{x^2-y^2}$ orbital occupancy.

A comparison of the structures of Co(F_{28}TPP)·2tol and Zn(F_{28}TPP)·THF reveals the stereochemical consequences of metal atom exchange. The perfluorinated porphyrin contracts around the smaller cobalt ion by shortening $C_\alpha-C_m$ and $C_\beta-C_\beta$ while keeping the other bond lengths constant. This type of distortion mitigates the steric interactions of the aryl C(11) and C(21) atoms with the β-fluorines, where the average distance for the C−F nonbonded contacts is 2.73 Å (versus 2.77 Å for Zn(F_{28}TPP)·THF). Presumably there is some limit to strain relief for this distortion mode, at which point the porphyrin core will adopt a nonplanar conformation if the ionic radius of the metal atom is sufficiently small; recent crystal structures of Zn(F_8TPP)·H_2O and Zn(F_8TPP)·THF support the suggestion that nonplanar conformations are easily accessed in β-octafluoro-*meso*-tetraarylporphyrins.[7,8]

Although the data are somewhat limited, an interesting trend emerges from inspection of Table 2: the core size of planar cobalt porphyrins is correlated with the presence of electron-withdrawing groups on the macrocycle. The same trend holds in planar zinc porphyrins.[7] Qualitative observations indicate that core contraction in nonplanar porphyrins is correlated with increased nitrogen basicity.[32] The current data suggest that radial expansion in planar porphyrins and nitrogen basicity are also correlated functions; substituents that decrease nitrogen basicity may expand the metalloporphyrin core. This proposed stereoelectronic relationship could resolve an apparent paradox concerning heme function: how does the porphyrin dilate to accept an in-plane, high-spin iron center and simultaneously remain a moderate field ligand? If nitrogen basicity decreases symbiotically with core expansion, no paradox exists.

Structure of Co(F_{28}TPP)·2THF. Crystals of Co(F_{28}TPP)·2THF suitable for X-ray diffraction were grown from THF. Two additional, disordered molecules of THF are incorporated within the crystal lattice (data not shown). A perspective drawing obtained from the crystal structure determination is shown in Figure 2, selected average bond lengths and angles are given in Table 1, and structural benchmarks are listed in Table 2. The macrocycle is essentially flat; no atom is displaced more than 0.06 Å from the mean porphyrin plane.

This crystal structure is the first bis(tetrahydrofuran) complex obtained for a Co(II) porphyrin. Generally, binding of a second axial ligand to Co(II) porphyrins such as Co(TPP) is weak; however, the extremely electron-deficient nature of F_{28}TPP stabilizes the six-coordinate complex (vide infra). The two exogenous ligands are bound tightly to the metal in Co(F_{28}TPP)·2THF; the Co−O bond lengths (2.204(2) Å) are shorter than those seen in diamagnetic Zn(TPP)·2THF (Zn−O = 2.380(2) Å)[27] or the high-spin iron complex Fe(TPP)·2THF (Fe−O = 2.351(3) Å).[29] The short Co−O bond length is attributable to two factors: (1) the reduced basicity of the coordinating nitrogen atoms in the heavily fluorinated porphyrin; (2) macrocycle core expansion which further attenuates σ-electron donation from nitrogen to cobalt.

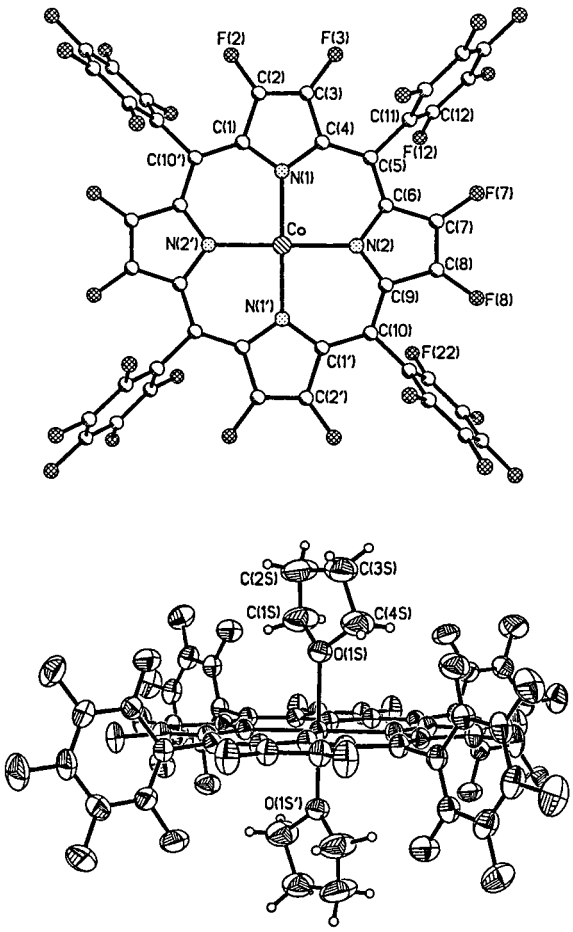

Figure 2. Perspective drawings from the X-ray crystal structure determination of Co(F_{28}TPP)·2THF. The bottom figure is drawn with 50% thermal ellipsoids.

The core size of Co(F_{28}TPP)·2THF is expanded in comparison to Co(F_{28}TPP)·2tol; the Co−N bonds are 0.082 Å longer in Co(F_{28}TPP)·2THF. This large change in metal nitrogen bond distance signifies a metal spin-state transition, since population of the $d_{x^2-y^2}$ orbital results in an antibonding metal−nitrogen interaction.[2] The core expansion observed upon binding of two THF molecules to Co(F_{28}TPP) is larger than that observed for the ($S = 0 \rightarrow S = 2$) spin transition in planar Fe(TPP) complexes (0.058 Å, Table 2)[29] and is of the same magnitude as that observed for the ($S = 0 \rightarrow S = 1$) spin transition in planar Ni(II) porphyrins (0.8 Å).[33] Thus, the structural data provide compelling evidence for exogenous ligand-dependent Co(II) spin-state modulation.

Axial Ligation. Association constants for exogenous ligand coordination to Co(F_8TPP) and Co(F_{28}TPP) were measured by visible spectroscopy. Methylene chloride solutions of the cobalt complexes were titrated with pyridine, THF, or MeIm; representative spectra are given in Figure 3. Clean isosbestic behavior was observed in all cases until the concentration of added ligand reached approximately 10 vol %. As expected, the electron-deficient octafluorinated porphyrins bind pyridine more tightly than Co(TPP) derivatives. For Co(*p*-X-TPP), binding of one pyridine is well modeled by a Hammett linear free energy relationship ($\log(K_X/K_H) = 4\sigma\rho$, $\sigma = \sigma_p$, $\rho = 0.168$),[34] and axial ligation is correlated with porphyrin ring

(31) Scheidt, W. R.; Turowska-Tyrk, I. *Inorg. Chem.* **1994**, *33*, 1314−1318.
(32) Barkigia, K. M.; Berber, M. D.; Fajer, J.; Medforth, C. J.; Renner, M. W.; Smith, K. M. *J. Am. Chem. Soc.* **1990**, *112*, 8851−8857.
(33) Kirner, J. F.; Garofalo, J. J.; Scheidt, W. R. *Inorg. Nucl. Chem. Lett.* **1975**, *11*, 107−112.
(34) Walker, F. A.; Beroiz, D.; Kadish, K. M. *J. Am. Chem. Soc.* **1976**, *98*, 3484−3489.

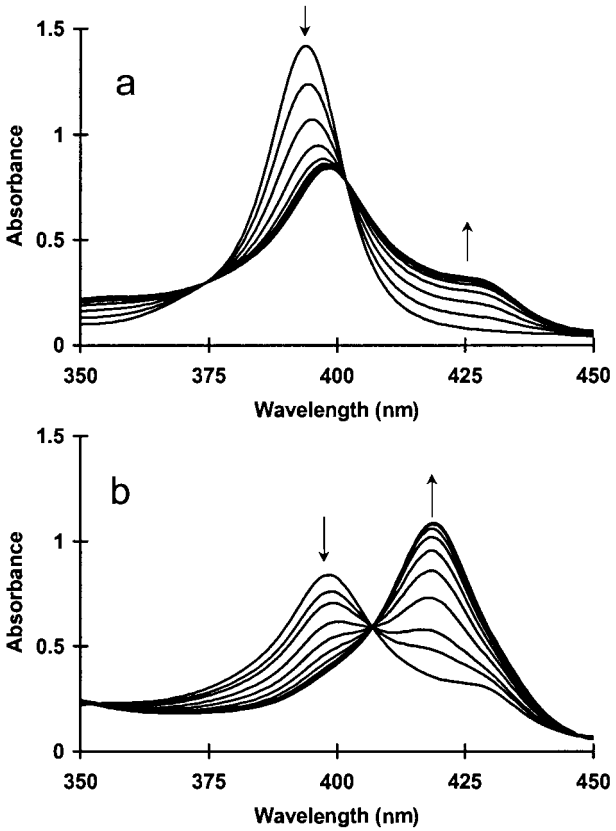

Figure 3. Titration of Co(F_{28}TPP) (6.95×10^{-6} M) in CH_2Cl_2 with 1-methylimidazole: (a) changes in the Soret region during the transition between 4- and 5-coordinate cobalt, 0 M < [MeIm] < 3.4×10^{-5} M; (b) changes in the Soret region during the transition between the 5- and 6-coordinate species, 3.4×10^{-5} M < [MeIm] < 2.1 M.

electrochemical potentials. The formation constants for pyridine ligation to Co(F_8TPP) ($\log(K_1) = 4.3$, $\log(K_2) = -0.08$) in CH_2Cl_2 compare with Co(TPP) ($\log(K_1) = 2.9$) and Co((CN)$_4$TPP) ($\log(K_1) = 4.2$, $\log(K_2) = -0.35$)[35] measured under identical conditions. Perhaps surprisingly, four β-cyano groups ($F = 0.51$) have an effect comparable to eight β-fluorine substituents ($F = 0.45$) for this reaction, despite the similar σ electron-withdrawing abilities of the two groups, as measured by the inductive substituent parameter, F.[36] Electrochemical data indicate that the porphyrin π-system of Zn(F_8TPP) is considerably more electron poor than Zn((CN)$_4$TPP).[7,35,37] Thus, Co(F_8TPP) is expected to be a significantly better σ-acceptor and a poorer π-donor toward pyridine than is Co((CN)$_4$TPP). The different σ and π energetic contributions to ligand association appear to cancel fortuitously in this case, leading to very similar formation constants.

Co(F_{28}TPP) binds axial ligands with the highest formation constants reported for a Co(II) porphyrin. Pyridine ($\log(K_1) = 5.9$, $\log(K_2) = 1.03$) and MeIm ($\log(K_1) = 6.8$, $\log(K_2) = 1.76$) bind avidly to the electron-deficient cobalt center. The large difference in the equilibrium constants for the first and second ligand additions (consistent with a half-filled metal d_{z^2} orbital) permits independent study of the five- and six-coordinate complexes in solution.

Table 3. ^{19}F NMR Chemical Shifts (ppm) of Fluorinated Porphyrin Derivatives[a]

compd[b]	β-F	*ortho*-F	*meta*-F	*para*-F
Co(F_8TPP)	−116.8			
Zn(F_8TPP)	−143.3			
Co(F_8TPP)·pyridine	−117.0			
Co(F_8TPP)·2pyridine[c]	−64.4			
Co(F_{28}TPP)	−124.8	−135.9	−160.4	−149.2
Zn(F_{28}TPP)	−145.4	−139.6	−161.9	−150.7
Co(F_{28}TPP)·pyridine	−104.6	−136.7	−161.2	−150.3
Co(F_{28}TPP)·2pyridine[c]	−20.5	−140.1	−163.5	−151.7
Co(F_{28}TPP)·2THF[d]	−1.6	−142.7	−165.6	−154.2
Co(F_{28}TPP)·2MeIm	+141.1	−146.6	−166.6	−155.6
Co(TPFPP)		−133.4	−160.4	−150.6
Zn(TPFPP)[e]		−138.5	−163.7	−154.8
Fe(TPFPP)·(3-F-pyridine)[f]		−138.1	−162.1	−152.1
Fe(TPFPP)(Cl)[e]		−105.8, −107.7	−153.9, −156.0	−150.2

[a] ^{19}F NMR values are reported relative to $\delta(CFCl_3) = 0$ ppm. The solvent was $CDCl_3$, unless otherwise indicated. [b] Abbreviations are listed in ref 1. [c] In pyridine-d_5. [d] In neat THF. [e] Data from ref 11 (in acetone-d_6). [f] Data from ref 41 (in benzene-d_6).

NMR Studies of Spin-State Modulation. Solution ^{19}F NMR investigations were performed in an effort to observe the ($S = {}^1/_2 \rightarrow S = {}^3/_2$) spin transition connoted by the structural studies. Typical Co(II) porphyrins show small contact shifts (1−3 ppm) and moderate dipolar shifts (6−8 ppm) for the porphyrin ring β-protons, regardless of axial ligation.[38] The ^{19}F NMR data for Co(F_8TPP), Co(F_{28}TPP), and relevant reference compounds are summarized in Table 3. The β-perfluorinated derivatives show substantial isotropic shifts (+20 ppm) for the porphyrin ring fluorines when only solvent molecules ($CDCl_3$) are available for axial coordination. The large difference in isotropic shifts between the porphyrin β-F resonances and the aryl (^{19}F or ^{1}H) resonances confirms that the anomalous β-F shifts are primarily contact in origin.[39] Solution magnetic susceptibility measurements (Evans' method, $CDCl_3$, 25 °C)[40] for Co(F_{28}TPP) gave $\mu_{eff} = 2.15\ \mu_B$. At elevated temperature μ_{eff} *increases*, consistent with thermal population of a high-spin excited state for Co(F_{28}TPP). With increasing pyridine concentration, the β-F chemical shift of Co(F_{28}TPP) gradually moves further downfield.

The five-coordinate pyridine adduct displays an intermediate contact shift for the β-fluorines (+40 ppm) and an intermediate magnetic moment, $\mu_{eff} = 2.82\ \mu_B$. There was no change (within experimental error) in the effective magnetic moment over the temperature range 20−60 °C. Under these conditions ligand loss and thermal population of the high-spin state compete. At room temperature Co(F_{28}TPP)·pyridine exhibits three broad resonances for the pentafluorophenyl groups. Below −20 °C, axial ligand exchange is slow on the NMR time scale, and five well-resolved aryl signals are observed. Variable-temperature ^{19}F NMR experiments ($CDCl_3$) of Co(F_{28}TPP)·pyridine yielded the activation parameters $\Delta H^{\ddagger} = 15.6$ kcal/mol and $\Delta S^{\ddagger} = 15$ eu for ligand dissociation. This value for $\Delta S^{\ddagger}$ compares with $\Delta S^{\ddagger} = 16$ eu for Co(*p*-OMeTPP) for loss of pyridine;[34] the nearly identical entropy values indicate that steric effects and the mode of binding are not drastically different for fluorinated and nonfluorinated porphyrins.

The ^{19}F NMR spectrum of the six-coordinate complex, Co(F_{28}TPP)·2pyridine, displays an exceptionally pronounced

(35) Lin, X. Q.; Boisselelier-Cocolios, B.; Kadish, K. M. *Inorg. Chem.* **1986**, *25*, 3242−3248.
(36) Hansch, C.; Leo, A.; Taft, R. W. *Chem. Rev.* **1991**, *91*, 165−195.
(37) Giraudeau, A.; Callot, H. J.; Jordan, J.; Ezhar, I.; Gross, M. *J. Am. Chem. Soc.* **1979**, *101*, 3857−3862.
(38) La Mar, G. N.; Walker, F. A. *J. Am. Chem. Soc.* **1973**, *95*, 1790−1796.
(39) La Mar, G. N.; Walker, F. A. *J. Am. Chem. Soc.* **1973**, *95*, 1782−1790.
(40) Evans, D. F. *J. Phys. Chem.* **1959**, *63*, 2004.

contact shift; the β-fluorines resonate 120 ppm downfield from the analogous signals in Zn(F_{28}TPP). For Co(F_{28}TPP)·2pyridine, a high-spin state ($S = {}^3/_2$) was confirmed by Evans' method (pyridine-d_5, $\mu_{eff} = 3.82\ \mu_B$). Other axial ligands, such as THF, also give high-spin complexes of Co(F_{28}TPP) at high (2 M) concentrations. Unfortunately, in all cases, the temperature dependence of the magnetic susceptibility could not be accurately determined because solubility and ligand binding were appreciably temperature dependent.

Two chemically reasonable Co(II) electronic configurations could lead to large isotropic shifts: $[(d\pi)^4(d_{xy})^1(d_{z^2})^1(d_{x^2-y^2})^1]$ ($^4A_{2g}$) or $[(d_{xy})^2(d\pi)^3(d_{z^2})^1(d_{x^2-y^2})^1]$ (^4E_g). The relative energies of these states should depend on the nature of the coordinating ligand. Strong σ-donor and π-donor ligands are expected to favor the latter ^4E_g state. The similar chemical shifts noted for six-coordinate THF and pyridine complexes of Co(F_{28}TPP) suggest that the π-bonding of pyridine is not playing a significant role and that the most likely ground state for these two complexes is ^4E_g. Unfortunately, there are no Co(II) standards with which the observed ^{19}F chemical shifts can be gauged. An estimation of the sensitivity of ^{19}F NMR to electron spin density can be made by comparing the NMR spectra of fluorinated and nonfluorinated paramagnetic compounds.[42] The β-fluorinated derivative 2-fluoro-3,8-diethyl-7,12,13,17,18-pentamethylporphyrin, FDEPMP, exhibits ^{19}F chemical shifts of -147, -148.5, -103, and 151 ppm for the free base, zinc complex, and the low- and high-spin iron(III) complexes, respectively.[43] The 254 ppm ^{19}F isotropic shift between the low- and high-spin complexes is roughly 2.5 times that seen for β-protons in ^{1}H NMR spectra of low- and high-spin Fe(III) tetraarylporphyrins.[44] This conversion factor is a convenient yardstick to compare contact shifts in the fluorinated cobalt porphyrins with proton paramagnetic shifts. Thus, the observed $\sim$120 ppm ^{19}F isotropic shift for β-fluorines in Co(F_{28}TPP) upon axial ligation approximately corresponds to a $\sim$50 ppm ^{1}H NMR isotropic shift for β-protons in tetraaryl derivatives. This downfield contact shift is of similar magnitude to that observed in planar, six-coordinate, high-spin Ni(II) porphyrins ($\sim$40$-$50 ppm)[33,45] and is consistent with placement of unpaired spin density in the $d_{x^2-y^2}$ orbital. The smaller size of Ni(II) (compared to Co(II)) makes direct computation of the degree of spin delocalization in Co(F_{28}TPP) impossible.

The magnitudes of the contact shifts observed upon axial coordination of Co(F_8TPP) are much smaller than those observed in Co(F_{28}TPP) (Table 3). The ^{19}F NMR spectrum of the five-coordinate complex Co(F_8TPP)·pyridine is essentially unshifted from that of Co(F_8TPP). The intermediate ^{19}F chemical shift observed for Co(F_8TPP)·2pyridine is consistent with a stronger ligand field provided by Co(F_8TPP) (compared to Co(F_{28}TPP)) and thermal population of the high-spin state. As with Co(F_{28}TPP), large isotropic shifts are only observed upon coordination of the sixth ligand. In principle, coordination by a fifth ligand could be expected to reduce substantially the energy of $d_{x^2-y^2}$ by lifting the metal atom from the porphyrin plane. However, this mechanism for lowering the $d_{x^2-y^2}$ orbital energy does not seem to be operative, because only the six-coordinate species exhibit large contact shifts. The studies with Co(F_8TPP) and Co(F_{28}TPP) indicate that a relatively small displacement of the Co(II) from porphyrin plane is caused by pyridine coordination, as is the case with other tetraarylporphyrins.[46] Clearly, ligand stereoelectronic features, rather than metal displacement, are responsible for the observed spin transitions.

Coordination by 1-methylimidazole (MeIm), a stronger σ-donor and stronger π-donor ligand than pyridine,[47] should raise the energy of the metal-centered dπ orbitals, resulting in complete conversion to the ^4E_g electronic state for the cobalt center in Co(F_{28}TPP). The ^{19}F NMR spectrum of the six-coordinate complex Co(F_{28}TPP)·2MeIm exhibits a dramatically larger isotropic shift (+286 ppm vs Zn(F_{28}TPP)) for the β-fluorines compared to the corresponding THF or pyridine adducts. The magnitude of this contact shift is comparable to that observed for high-spin Fe(FDEPMP)Cl (+299 ppm vs Zn(FDEPMP)) and is consistent with additional in-plane spin density and complete transfer of one electron to the $d_{x^2-y^2}$ orbital. For the $S = {}^1/_2 \rightarrow S = {}^5/_2$ transition of Fe(III), the net change in in-plane spin density is three unpaired electrons, while for the $^2A_{1g} \rightarrow {}^4E_g$ spin transition the net change is one electron. If the conformations for the two porphyrins were the same, one would expect a smaller isotropic shift for Co(F_{28}TPP)·2MeIm than Fe(FDEPMP)Cl. The cobalt atom of Co(F_{28}TPP)·2MeIm is expected to be in the plane of the porphyrin, maximizing σ-spin delocalization, but the displacement of the high-spin iron from the porphyrin plane reduces σ-spin density and increases π-spin delocalization, complicating any direct comparison of chemical shift assignments for the cobalt and iron porphyrins. The magnitude of the isotropic shift in Co(F_{28}TPP)·2MeIm also parallels (with the conversion factor 2.5) the +125 ppm shift noted for the β-proton resonances in the ^{1}H NMR spectra of the Fe(TPP)X series along the $S = {}^3/_2 \rightarrow$ admixed $^3/_2$,$^5/_2 \rightarrow S = {}^5/_2$ spin continuum.[48] On the basis of this evidence we assign the ^4E_g ground state for Co(F_{28}TPP)·2MeIm. This complex is the first example of a high-spin Co(II) in a porphyrin ligand.

Summary and Conclusion

The structural and ^{19}F NMR data presented here indicate that β-octafluorination of porphyrins results in a substantially reduced crystal field for chelated cobalt, yielding the first examples of high-spin Co(II) porphyrins. The X-ray crystal structure determination of Co(F_{28}TPP)·2THF shows a porphyrin possessing a substantially dilated porphyrin core, and ^{19}F NMR experiments with Co(F_{28}TPP) show pronounced, axial ligand-dependent downfield shifts for the porphyrin β-fluorine resonances. These data are consistent with population of the $d_{x^2-y^2}$ orbital of the metal center and a ^4E_g electronic configuration.

The reduced ligand field of Co(F_{28}TPP) permits variable spin-state behavior and thereby mimics many of the essential electronic features of hemes without extrusion of the metal center from the porphyrin plane. These features include modulation of spin state by axial ligation, thermal population of high-spin states, and radial core expansion to accommodate a high-spin ion. Therefore, heavily fluorinated cobalt porphyrins are interesting model systems for investigating stereoelectronic

(41) Moore, D. T.; Horváth, I. T.; Therien, M. J. *J. Am. Chem. Soc.* **1997**, *119*, 1791−1792.
(42) Mascharak, P. K.; Smith, M. C.; Armstrong, W. H.; Burgess, B. K.; Holm, R. H. *Proc. Natl. Acad. Sci. U.S.A.* **1982**, *79*, 7056−7060.
(43) Suzuki, A.; Toi, H.; Aoyama, Y.; Ogoshi, H. *Heterocycles* **1992**, *33*, 87−90.
(44) La Mar, G. N.; Walker, F. A. In *The Porphyrins*; Dolphin, D., Ed.; Academic Press: New York, 1979; Vol. IVB, pp 61−158.
(45) Ozette, K.; Leduc, P.; Palacio, M.; Bartoli, J.-F.; Barkigia, K. M.; Fajer, J.; Battioni, P.; Mansuy, D. *J. Am. Chem. Soc.* **1997**, *119*, 6442−6443.
(46) Walker, F. A. *J. Am. Chem. Soc.* **1973**, *95*, 1150−1153.
(47) Chacko, V. P.; La Mar, G. N. *J. Am. Chem. Soc.* **1982**, *104*, 7002−7007.
(48) Reed, C. A.; Guiset, F. *J. Am. Chem. Soc.* **1996**, *118*, 3281−3282.

effects in hemes. Finally, the tendency for high-spin states to be favored in octafluorometalloporphyrins should extend to other metals in the first transition series. Thus, the chemistry of known intermediate- and high-spin states of iron porphyrins can be explored with novel axial ligands.

Experimental Section

Instrumentation and Materials. Manipulations of air- and water-sensitive reagents were carried out either in a glovebox (Innovative Technologies Labmaster 150) or in standard Schlenk-style glassware. Solvents used in the glovebox were degassed at least three times by successive freeze/pump/thaw cycles. THF was distilled from sodium/benzophenone prior to use. Methylene chloride was distilled from CaH_2 under nitrogen. Benzonitrile, pyridine, and deuterated solvents were distilled from CaH_2 under vacuum. Cobalt chloride was dried under vacuum and stored in the glovebox. The remaining reagents were obtained from Aldrich or Fisher chemical companies and used as received. Optical spectra were performed using an OLIS-14 modification of a Carey-14 UV−vis−NIR spectrophotometer equipped with a variable-temperature cell holder and a circulating VT bath (Laude RC3). Binding constants were calculated using the curve-fitting routines supplied in the Olis software package. NMR spectra were obtained in the instrumentation center at the University of Nebraska—Lincoln using 360 or 500 MHz spectrometers. Proton NMR spectra were collected in $CDCl_3$ or pyridine-d_5 using the residual protons in the solvents as a chemical shift references. ^{19}F NMR was conducted at 470 MHz, and chemical shifts are given with reference to an added internal standard, $CFCl_3$. The data sets for the crystal structure analyses were collected at the University of Illinois crystallography facility. Quantitative Technologies Inc., Whitehouse, NJ, conducted the combustion analyses.

[2,3,7,8,12,13,17,18-Octafluoro-5,10,15,20-tetraphenylporphinato]-cobalt(II), Co(F_8TPP). Under N_2, a solution of 2,3,7,8,12,13,17,18-octafluoro-5,10,15,20-tetraphenylporphyrin (104 mg, 0.137 mmol) and $CoCl_2$ (178 mg, 1.370 mmol) in THF (80 mL) was charged with Li(HMDSA) (0.3 mL of a 1.0 M THF solution) and stirred for 12 h. The reaction mixture was partitioned between water and diethyl ether. The organic layer was washed (3 × 100 mL) with water, dried over Na_2SO_4, and evaporated. The isolated brown solid was dried *in vacuuo* and recrystallized from hot toluene, yielding brown needles (82 mg, 0.101 mmol, 73%). For analytical, NMR, and optical experiments the crystalline material was dried under vacuum at 110 °C for 12 h. ^1H NMR (500 MHz, $CDCl_3$): δ 12.4 (broad s, 8 H), 9.7 (broad s, 8 H), 9.5 (broad s, 4 H). ^{19}F NMR (470 MHz, $CDCl_3$): δ −116.81 (broad s, 8 F). UV−vis (CH_2Cl_2): 398 (5.34), 519 (4.12). FAB-MS (*m*/*e*): low res, 815.1 (calcd 815.6); high res, 815.0871, 816.0928 (calcd 815.08922, 816.09258). Anal. Calcd for $C_{44}H_{20}F_8N_4Co$: C, 64.80; H, 2.47; N 6.87. Found: C, 64.53; H, 2.38; N, 6.75.

[2,3,7,8,12,13,17,18-Octafluoro-5,10,15,20-tetrakis(pentafluorophenyl)porphinato]cobalt(II), Co(F_{28}TPP). Under N_2, 50 mL of a THF solution containing 2,3,7,8,12,13,17,18-octafluoro-5,10,15,20-tetrakis-(pentafluorophenyl)porphyrin (102 mg, 0.091 mmol) and $CoCl_2$ (118 mg, 0.910 mmol) was treated with Li(HMDSA) (0.2 mL of a 1.0 M THF solution). Metalation commenced immediately and was complete within 10 min. The reaction mixture was partitioned between water and diethyl ether. The organic layer was washed (3 × 100 mL) with water, dried over Na_2SO_4, and evaporated. The isolated deep red solid was dried under vacuum and recrystallized from hot toluene yielding deep red hexagonal crystals (79 mg, 0.067 mmol, 74%). These crystals were suitable for X-ray diffraction. For analytical, NMR, and optical experiments the crystalline material was dried under vacuum at 110 °C for 12 h. ^{19}F NMR (470 MHz, $CDCl_3$): δ −124.8 (s, 8F), −135.9 (s, 8F), −149.2 (s, 4F), −160.4 (s, 8F) (all signals broad). UV−vis (CH_2Cl_2): 394 (5.31), 520 (4.06). FAB-MS (*m*/*e*): low res, 1175.1 (calcd 1174.9); high res, 1174.9040, 1175.9084 (calcd 1174.9007, 1175.9041). Anal. Calcd for $C_{44}F_{28}N_4Co$: C, 44.96; N 4.77. Found: C, 44.36; N 4.68.

Formation Constant Measurements. Solutions of Co(F_8TPP), Co(F_{28}TPP), pyridine, *N*-methylimidazole, and THF in CH_2Cl_2 were prepared in an inert atmosphere glovebox. For each experiment, a sample solution of Co(F_8TPP) or Co(F_{28}TPP) (10.000 mL) was placed into a thermostated Schlenk-style quartz cell (1.00 cm) and the concentration (4×10^{-6}−7×10^{-6} M) was determined spectrophotometrically. The porphyrin solution was first titrated with dilute pyridine, *N*-methylimidazole, or THF solutions (1×10^{-3} M in CH_2Cl_2) to obtain K_1. For measurements of K_2 the neat ligands were added. All manipulations were carried out in the glovebox. The resulting series of spectra was corrected for concentration changes, and equilibrium constants were extracted by curve fitting the Soret region using standard spectra of 4-, 5-, and 6-coordinate species. The Olis software package was used to perform the data analysis.

X-ray Crystal Structure Determination of Co(F_{28}TPP)·2tol. Single crystals of $Co[N_4C_{44}F_{28}][C_6H_5CH_3]_2$ are, at −75 ± 2 °C, monoclinic, space group $C2/c$-C_h (No. 15) with a = 22.1616(5) Å, b = 12.0274(3) Å, c = 19.9159(2) Å, β = 110.645(1)°, V = 4967.6(2) Å^3, and Z = 4 {d_{calcd} = 1.818 g/cm^3; μ_a(Mo Kα) = 0.50 mm^{-1}}. A full hemisphere of diffracted intensities (ω scan width of 0.30°) was measured using graphite-monochromated Mo Kα radiation on a Siemens SMART CCD area detector. X-rays were provided by a normal focus sealed X-ray tube operated at 50 kV and 40 mA. Lattice constants were determined with the Siemens SMART/SAINT software package using peak centers for 5835 reflections. A total of 16 059 integrated reflection intensities having 2θ(Mo Kα) < 56.55° were collected using the Siemens program SAINT. A total of 5981 of these were independent and gave R_{int} = 0.035. The Siemens SHELXTL-PC Version 5 software package was used to solve and refine the structure. "Direct methods" techniques were used to solve the structure, and all stages of weighted full-matrix least-squares refinement were conducted using F_o^2 data. The structure refinement converged to give R_1 (unweighted, based on F) = 0.035 for 4045 independent absorption-corrected reflections having 2θ(Mo Kα) < 56.55° and $I > 2\sigma(I)$ and wR_2 (weighted, based on F^2) = 0.124 for all 5981 independent absorption-corrected reflections having 2θ(Mo Kα) < 56.55°. The structural model incorporated anisotropic thermal parameters for all non-hydrogen atoms and fixed isotropic thermal parameters for hydrogen atoms of the toluene molecules. These hydrogen atoms were included in the structure factor calculations as idealized atoms (assuming sp^3- or sp^2-hybridization of the carbon atoms and C−H bond lengths of 0.95 Å) "riding" on their respective carbon atoms; their isotropic thermal parameters were fixed at values 1.2 (aromatic) or 1.5 (methyl) times the equivalent isotropic thermal parameters of the carbon atoms to which they are covalently bonded.

X-ray Crystal Structure Determination of Co(F_{28}TPP)·2THF. Single crystals of $[OC_4H_8]_2Co[N_4C_{44}F_{28}]\cdot 2(OC_4H_8)$ at −75 ± 2 °C are triclinic, space group $P\bar{1}$ (No. 2) with a = 11.0691(1) Å, b = 12.0451(1) Å, c = 12.9558(2) Å, α = 62.531(1)°, β = 69.544(1)°, γ = 76.181(1)°, V = 1429.71(3) Å^3, and Z = 1 {d_{calcd} = 1.700 g/cm^3; μ_a(Mo Kα) = 0.45 mm^{-1}}. A full hemisphere of diffracted intensities (ω scan width of 0.20°) was measured using graphite-monochromated Mo Kα radiation on a Siemens/Bruker SMART CCD single-crystal diffraction system. X-rays were provided by a normal-focus sealed X-ray tube operated at 50 kV and 40 mA. Lattice constants were determined with the Siemens/Bruker SAINT software package using peak centers for 5354 reflections. A total of 9361 integrated reflection intensities having 2θ(Mo Kα) < 56.43° were produced using the Siemens/Bruker program SAINT. A total of 6487 of these were independent and gave R_{int} = 0.040. The Siemens/Bruker SHELXTL-PC software package was used to solve the structure with "heavy atom" techniques. All stages of weighted full-matrix least-squares refinement were conducted using F_o^2 data with the SHELXTL-PC Version 5 software package. Final agreement factors at convergence are the following: R_1 (unweighted, based on F) = 0.060 for 5262 independent absorption-corrected reflections having 2θ(Mo Kα) < 56.43° and $I > 2\sigma(I)$}, wR_2 (weighted, based on F^2) = 0.161 for 6067 independent absorption-corrected reflections having 2θ(Mo Kα) < 56.43° and $I > 0$; R_1 (unweighted, based on F) = 0.079, wR_2 (weighted, based on F^2) = 0.179 for all 6487 independent absorption-corrected reflections having 2θ(Mo Kα) < 56.43°.

The structural model incorporated anisotropic thermal parameters for all non-hydrogen atoms and isotropic thermal parameters for all hydrogen atoms. Methylene hydrogen atoms on the tetrahydrofuran molecules were included in the structural model as fixed atoms (using

idealized sp^3-hybridized geometry and a C−H bond length of 0.99 Å) "riding" on their respective carbons. Their isotropic thermal parameters were fixed at values 1.2 times the equivalent isotropic thermal parameter of the carbon atom to which they are covalently bonded.

Acknowledgment is made to the donors of the Petroleum Research Fund, administered by the American Chemical Society, for the support of this research. We also thank Professor Victor Day of this department for performing the crystal structure analyses of Co(F_{28}TPP)·2tol and Co(F_{28}TPP)·2THF and Crystalytics Co. of Lincoln, NE, for the use of its equipment and supplies for the structure analyses. We thank Professors Jody Redepenning and Richard Shoemaker for their assistance and helpful discussions. This work was also supported by the Center for Metallobiochemistry at the University of Nebraska.

Supporting Information Available: X-ray crystallographic data for Co(F_{28}TPP)·2tol and Co(F_{28}TPP)·2THF, including numbered figures and tables of crystal data, atomic coordinates, temperature factors, and bond lengths and bond angles (17 pages). Ordering information is given on any current masthead page.

IC980156O